The zinc–chlorine battery: half-cell overpotential measurements

J. JORNÉ, J. T. KIM,* D. KRALIK†

Department of Chemical and Metallurgical Engineering, Wayne State University, Detroit, Michigan 48202, USA

The voltaic performance of the zinc–chlorine battery was investigated by measuring the individual potentials of the Zn and Cl_2 electrodes versus a reference electrode. The overpotential at the Zn electrode is very small for both the charging and the discharging processes, and the use of a flow-through porous Cl_2 electrode is advantageous. Energy efficiency in the region of 65% has been achieved for a complete cycle. Tafel polarization data for both the zinc and the Cl_2/graphite electrodes was obtained using rotating zinc hemisphere and graphite disc electrodes. Exchange current densities and Tafel slopes are reported.

1. Introduction

The zinc–chlorine battery concept is based upon the electrochemical reaction between zinc, chlorine and $ZnCl_2$ aqueous solution, and the simultaneous chemical reaction between chlorine and water [1]. The overall reactions are:

$$ZnCl_{2(aq)} \rightleftarrows Zn_{(s)} + Cl_{2(g)}$$

$$Cl_{2(g)} + xH_2O \rightleftarrows Cl_2 \cdot xH_2O$$

$$x \simeq 5.9.$$
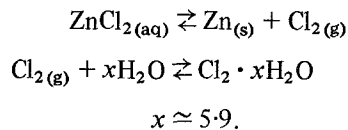
The reactions are highly reversible. The e.m.f. of a Zn–Cl_2 cell under standard conditions is 2·12 V. During the charging process, the $ZnCl_2$ electrolyte is electrolysed, yielding a zinc deposit on an inert graphite substrate and Cl_2 evolution on a porous flow-through graphite anode. The Cl_2 gas is removed from the cell to another chamber where it is mixed with water at approximately 10° C and chlorine hydrate is formed.

During the discharging process, chlorine is evolved by heating the chlorine hydrate, mixed with the $ZnCl_2$ electrolyte, and passing it through the porous graphite electrode. Chlorine is consumed electrochemically while zinc dissolves at the other electrode. Coulombic inefficiencies are due mainly to the chemical recombination of zinc with dissolved chlorine. It has been shown by Kim and Jorné [2] that this process is limited by the mass transfer of dissolved chlorine to the zinc electrode. The kinetics and mass transfer of the chlorine electrode on a rotating graphite electrode has been investigated by Kim and Jorné [3] and the kinetic parameters and a kinetic mechanism have been proposed.

In this paper the voltaic behaviour of a single cell is investigated and the individual overvoltages are measured using zinc or calomel reference electrodes. The reference electrode was located in a separate compartment and connected by a tube to the interelectrode space. It is shown that the overpotential at the zinc electrode is very small (< 50 mV) while the overpotential on the Cl_2 flow-through graphite electrode is about 100 mV. The ohmic drop can be decreased by adding KCl and NaCl as supporting electrolytes. Polarization data for the zinc electrode and Cl_2 electrode were obtained using a rotating zinc hemisphere and rotating graphite disc electrode, respectively.

2. Experimental

A single Zn–Cl_2 cell was used (EDA, Madison Heights, Michigan) [8]. The cell is shown in Fig. 1 and consists of a dense graphite electrode (Union Carbide ATJ Graphite) on which zinc is deposited,

* Present address: Bell Laboratories, Murray Hill, N.J. 07974.
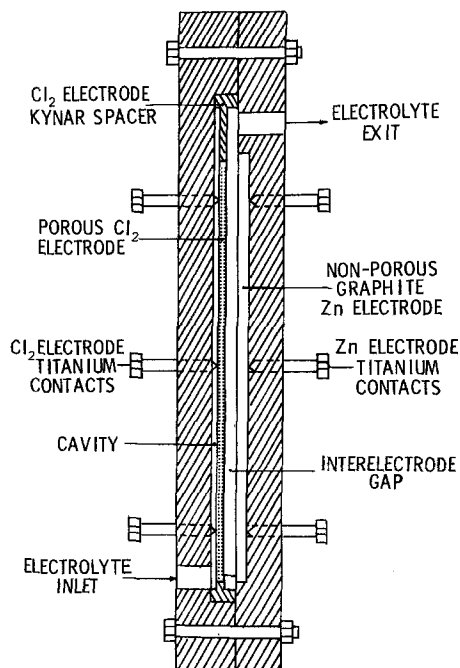† Present address: Diamond Shamrock Company, Painesville, Ohio 44070.

Fig. 1. The single cell (cross-section).

and a porous flow-through graphite electrode (Union Carbide Porous Graphite Grade 60) on which chlorine is evolved. The thickness of the porous graphite electrode is 0·2 cm and the porosity is 0·52. The gap between the two electrodes is 0·2 cm. The apparent active area of the electrodes was 68 cm^2, the total current was 3 A and the charging process lasted for 1–2 hours. The experimental set-up is shown in Fig. 2. A 2·5 ℓ ZnCl$_2$ (2 M) solution was circulated through a flow meter and the cell using a Kynar pump with a

teflon gear (EDA modified micropump). The flow rate was 60 ml min^{-1}. The evolved Cl$_2$ was stripped during the charging by nitrogen bubbling throughout the experiment. Prior to each experiment the pH was adjusted by adding HCl and nitrogen was bubbled to remove oxygen and the remaining dissolved chlorine. The charging time was adjusted so that the amount of electricity was always the same, 0·080 A h cm^{-2}. The zinc deposits were peeled gently off the graphite substrate, washed thoroughly, dried and weighed. The ZnCl$_2$ concentration was 2 M and in some cases KCl and NaCl supporting electrolytes were added in order to reduce the ohmic resistance. In some cases the ZnCl$_2$ concentration was reduced down to 0·5 M.

During the discharge of the cell, Cl$_2$ gas was bubbled through the electrolyte reservoir and fed to the cell with the flowing ZnCl$_2$ solution. The discharging lasted until the cell was completely exhausted and all the Zn deposit was redissolved.

The reference electrode consisted of a Zn rod or SCE placed in a separate compartment filled with the cell's ZnCl$_2$ solution. The reference electrode compartment was connected to the cell by a tube, and by small holes in the interelectrode spacing. The tops of the holes were located in the middle of the gap between the two graphite electrodes. The overpotentials were corrected for ohmic drop using the conductivities of the solutions.

The current was applied by an Udylite PC-10 constant current power supply. The potentials were measured by a Keithley 600 A electrometer and recorded on a multi-channel recorder (Honeywell Electronik 194) for the entire charging and
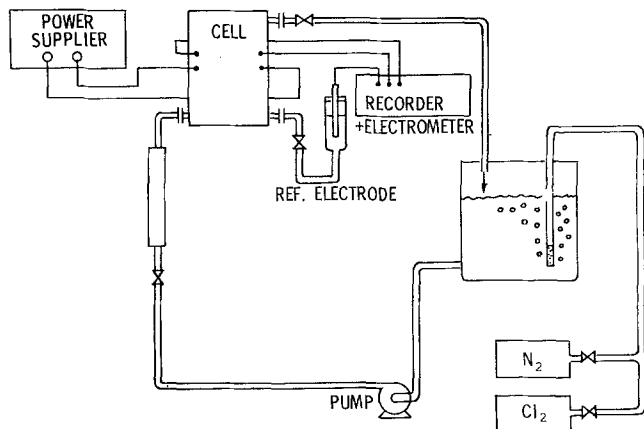

Fig. 2. The experimental system.

discharging of the cell. The amount of electricity passed was measured by an EDA digital coulometer and agreed well with the current–time measurements.

The rotating graphite disc electrode consists of a teflon support rod and a central dense graphite electrode (ATJ Union Carbide). The central graphite electrode was embedded in the teflon rod. The diameter of the graphite electrode was 0·95 cm and the diameter of the teflon rod was 1·9 cm. The rotator was Pine Instrument ASR rotator with a rotational speed of 0–10 000 rev min^{-1}. The surface of the electrode was polished with waterproof Al_2O_3 paper and a fine paper using the rotator ($\omega = 4000$ rev min^{-1}).

A 1000 ml pyrex vessel fitted with a teflon cover was used as the cell container. It was equipped with a 2·25 cm^2 platinum counter electrode compartment connected to the cell by a small glass tube. A saturated calomel electrode (SCE) served as a reference electrode and was placed in a separate reference electrode's compartment connected to the main cell by a capillary extending to the side of the rotating disc electrode. The top of the luggin capillary was located at a distance of 3·5 cm from the centre of the disc. The ohmic drops were calculated according to Newman [4].

The potential of the graphite disc electrode was controlled by a Wenking LT 73 potentiostat. A wave-form generator (TWG 500) was used in con-junction with the potentiostat in order to sweep the potential of the disc electrode. The potential–current data were recorded on a Houston Instrument 2000 X–Y Recorder.

The $ZnCl_2$ solution was obtained from EDA, Inc. where it was prepared by direct recombination of Cl_2 gas and pure Zn rods (99·999% New Jersey zinc). The $ZnCl_2$ concentration was measured by hydrometer. Cl_2–N_2 gas mixtures were fed into the cell by a gas dispenser, and the dissolved Cl_2 concentration was maintained by measuring the Cl_2 and N_2 flow rates. The dissolved Cl_2 concentration was measured by standard titration using 0·01 N $Na_2S_2O_3 \cdot 5H_2O$. Dissolved oxygen was removed by bubbling N_2 prior to the experiments, and the Cl_2–N_2 gas mixture was bubbled throughout the experiments.

The polarization measurements of the zinc metal in zinc chloride solution were performed on a rotating hemispherical zinc electrode [3]. In order to eliminate the concentration overpotential, the rotational speed of the electrode was $\omega = 3000$ rev min^{-1}. Hemispherical electrode was used because its primary current distribution is uniform.

3. Results and discussion

3.1. Single cell

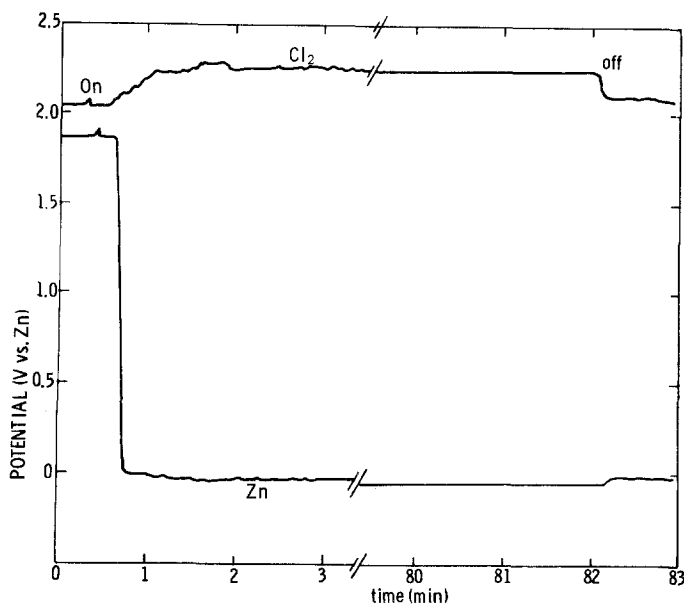The potentials of the zinc and the chlorine electrodes versus the zinc reference electrode were

Fig. 3. The potentials of the Cl_2 and Zn electrodes versus the Zn reference electrode during the charging. Electrolyte, $ZnCl_2$ (2 M); temperature, 25° C; total current, 3 A; apparent current density, 44 mA cm^{-2}; reference electrode, Zn.
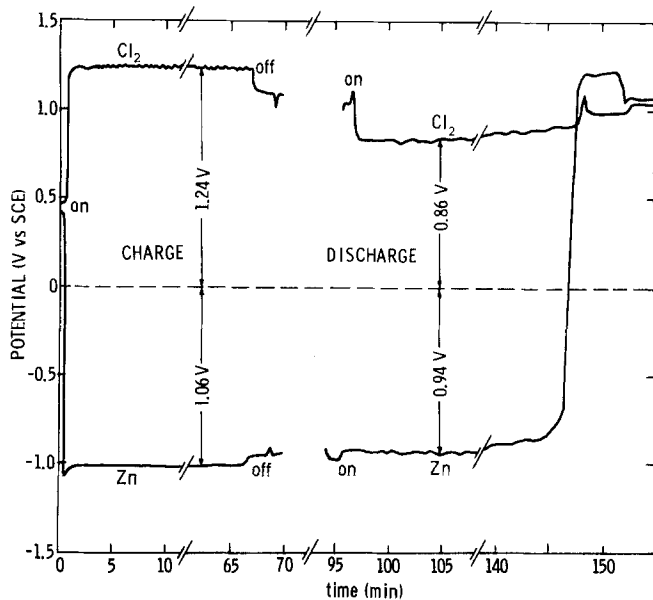
Fig. 4. The potentials of the Cl_2 and Zn electrodes versus SCE reference electrode during the charging and discharging cycle. Electrolyte, $ZnCl_2$ (2 M) + KCl (4 M); temperature, 25° C, pH = 0·1; total current 1·5 A; apparent current density, 22 mA cm^{-2} cm^{-2}; reference electrode, SCE; Cl_2 concentration during the discharging, 2·4 g l^{-1}.

measured during the charging and the discharging of the single cell. Typical charge and charge–discharge curves are shown in Figs. 3 and 4 for the charging and charging–discharging cycles, respectively. The upper curves show the Cl_2–porous graphite electrode potential, and the lower curves represent the Zn electrode potential versus the reference electrode. The overall cell potential is the difference between the two curves and is 2·30 V during the charging and 1·80 V during the discharging. The individual overvoltage can be read from the drop in the potential after the current is shut off. The main overpotential appears to be on the Cl_2 electrode. The overpotential on the Zn electrode is very small, below − 50 mV during charging and below + 40 mV during discharging. The overpotential on the Cl_2 electrode is + 100 mV and − 150 mV during charging and discharging, respectively. By adding KCl (2 M) and NaCl (2 M) as supporting electrolytes, the ohmic drop was reduced significantly and the overall cell potential was reduced to 2·20 V during the charging and increased to 1·90 V during the discharging. The voltaic performance of the cell improved by adding KCl both during charging and discharging; however, the addition of NaCl lowered only the charging voltage, but did not improve discharging voltage as expected from conductance measurements.

The source of the electrode overpotentials is mostly kinetic. Because of the high Zn^{2+} and Cl^- ionic concentrations, mass transfer overpotential is small during the charging process. Mass transfer overpotential can become significant only during the discharging process at the Cl_2 electrode. The solubility of Cl_2 in the solution is of the order of 0·01 M; however, the use of a flow-through porous electrode eliminates the significance of mass transfer overpotential. Kim and Jorne [3] measured the mass transfer and the kinetics of the cathodic reduction of dissolved Cl_2 and showed that the kinetics of the reaction are moderately fast ($i_0 = $ 1·1 mA cm^{-2}). Therefore, using a flow-through porous electrode ensures that mass transfer is not the rate-determining step during the discharging process. The overpotential of the Cl_2 electrode includes probably some ohmic drop within the porous structure.

A complete cycling of the single cell is shown in Fig. 4, where the potentials of the Zn and Cl_2 electrodes were measured versus SCE. The average charging voltage was 2·3 V and the average discharging voltage was 1·8 V. The voltaic efficiency is given by 1·8/2·3 × 100 = 78%. The coulombic efficiency was measured from the total charge passed during the charging and discharging process, 6000 and 5040 C, respectively. Hence, the coulombic efficiency is 5040/6000 × 100 = 84%. The

energy efficiency is given by

energy efficiency = (voltaic efficiency)

x (coulombic efficiency)

= 0·78 × 0·84 × 100 = 66%.

The overpotentials at the Zn electrode are − 50 mV and + 40 mV for the charging and discharging, respectively. The overpotentials at the Cl_2 electrode are + 120 mV and − 200 mV for the charging and discharging, respectively. At the end of the discharging process, all of the zinc is removed from the graphite substrate and Cl_2 is evolved and the recorded potential corresponds to that of the anode during the preceding charging process (see Fig. 4).

3.2. Tafel's kinetic parameters

The Tafel polarization data for Cl_2/Cl^- on a dense graphite electrode is shown in Fig. 5. The data was corrected for ohmic drop using Newman's method [4]. The apparent exchange current density, $i_0 = 1·1$ mA cm^{-2}, is obtained from the intercept of the cathodic and anodic polarization branches. The anodic and cathodic Tafel slopes are $b_a = 124$ and $b_c = − 120$ mV/decade, respectively. The present parameters are in agreement with the results of Hine [5] for NaCl solution ($i_0 = 1·2$ mA cm^{-2}, $b_a = − b_c = 120$ mV/decade). The deviation from linearity at the far cathodic potential range $E <$ 0·75 V versus SCE in Fig. 5 is due to the mass

transfer overpotential. Detailed studies of the kinetics of the Cl_2/graphite electrode in $ZnCl_2$ solution are presented by Kim and Jorné [2].

The Tafel polarization curves for the zinc electrode in various $ZnCl_2$ solutions are shown in Fig. 6. The data was corrected for ohmic drop using Newman's method [4] for the case where the reference electrode is located far away (3·50 cm):

$$R = \frac{1}{4\pi\kappa r}.$$

R is the resistance (Ω), κ is the conductivity (Ω^{-1}cm^{-1}) of the solution and r is the radius of the electrode (cm). The conductivities of the 0·5, 1·0 and 2·0 M $ZnCl_2$ solutions are 0·0820, 0·0943 and 0·0980 Ω^{-1} cm^{-1}, respectively. The obtained exchange current densities and anodic and cathodic Tafel slopes are summarized in Table 1. The theoretical cathodic Tafel slope is $b_c = − − [2·3RT/(1 − \beta)nF]$. If a symmetric transfer coefficient $\beta = 0·5$ and one electron transfer $n = 1·0$ are assumed, then the Tafel slope is $b_c = − 120$ mV. The obtained experimental cathodic Tafel slopes (see Table 1) are in agreement with the theoretical value. Sierra Alcazar and Harrison [6] measured a Tafel slope of 120 mV using an a.c. impedence technique.

The exchange current density (i_0) was calculated from the intercepts of the anodic and the cathodic branches in Fig. 6, and the obtained data is also summarized in Table 1. The kinetics of the
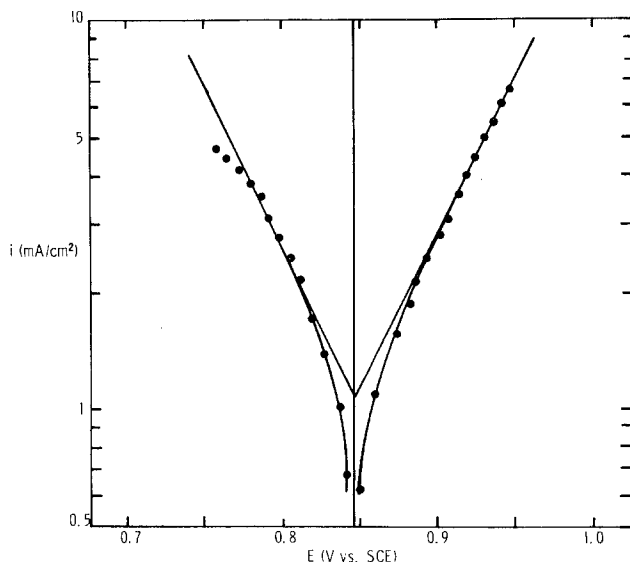

Fig. 5. Anodic and cathodic Tafel polarizations of rotating graphite disc electrode in 37 wt% $ZnCl_2$ solution. $[Cl_2] = 1·17$ g l^{-1}. Area = 0·713 cm^2, pH = 3·29, rotational speed = 3000 rev min^{-1}.
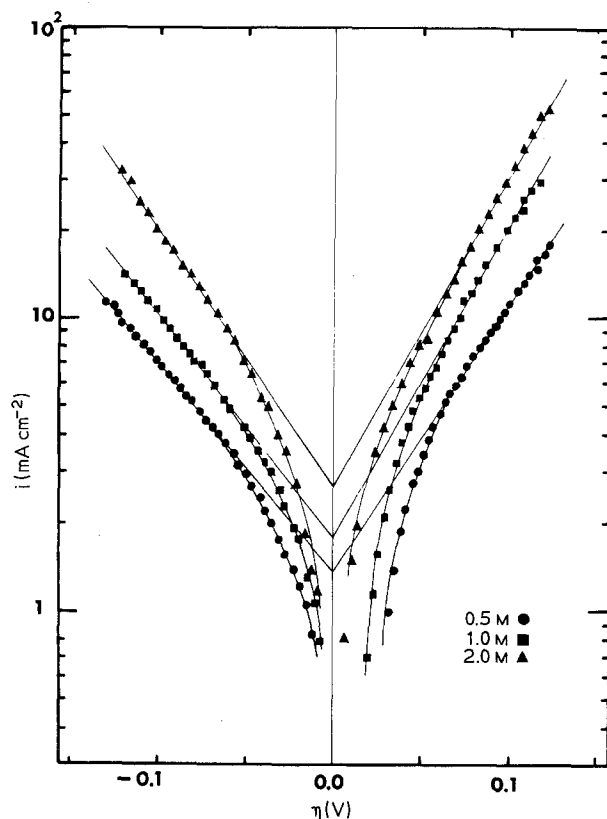
Fig. 6. Anodic and cathodic Tafel polarizations of rotating Zn hemispherical electrode in various $ZnCl_2$ and 1 M KCl solutions. Area = 0·752 cm^2, rotational speed = 3000 rev min^{-1}.

Zn electrode are quite fast. The exchange current density of Zn/Zn^{2+} in KCl is reported by Sierra Alcazar and Harrison [6]: $i_0 = 0.52$ mA cm^{-2} for 10^{-2} M $ZnSO_4$ + 1·0 M KCl (pH = 3·5). However, the exchange current also varies with the pH: 1·1 and 0·98 mA cm^{-2} in pH of 3 and 1·8, respectively, Detailed kinetics studies and mass transfer of zinc electrode in $ZnCl_2$ solutions are given by Kim [7].

4. Conclusions

The voltaic performance of the Zn–Cl$_2$ battery was investigated. Flat charge/discharge curves were

observed. The main overvoltage was detected on the Cl$_2$ electrode, while the Zn overvoltage was very low for both the charging and discharging steps. It is believed that most of the Cl$_2$ electrode overpotential is kinetic and includes some ohmic drop within the porous structure. The ohmic drop can be reduced by adding KCl or NaCl supporting electrolytes; however, NaCl was found to be inefficient in improving the discharging cell voltage. The use of a porous flow-through graphite electrode is essential because of the low solubility of Cl$_2$ and the otherwise build-up of mass transfer overpotential during the discharging of the cell. Tafel kinetics have been observed for both chlorine and zinc electrodes and their exchange current densities are in the several mA cm^{-2} range.

Table 1. The kinetic parameters of the zinc electrode in ZnCl$_2$ solution (pH = 2·0)

$ZnCl_2$ (M)	i_0 (mA cm^{-2})	b_a (mV)	$-b_c$ (mV)
0·5	1·36	108·5	139·5
1·0	1·75	94·4	131·3
2·0	2·65	90·6	113·7

References

[1] P. C. Symons and P. Carr, *Proceedings of the 8th Inter-society Energy Conversion Engineering Conference*, (1973) Paper No. 739010, pp. 72–77.

[2] J. T. Kim, and J. Jorné, *J. Electrochem. Soc.* **124** (1977) 1473.

[3] *Idem, ibid* **125** (1978) 89.

[4] J. Newman, *ibid* **113** (1966) 501.

[5] F. Hine and M. Yasuda, *ibid* **121** (1974) 1289.

]6] H. B. Sierra Alcazar and J. A. Harrison, *Electrochim. Acta* **22** (1977) 627.

[7] J. T. Kim, PhD dissertation, Wayne State University, Detroit, Michigan (1978).

[8] D. Kralik, MS thesis, Wayne State University, Detroit, Michigan (1978).